

Multiuser quantum communication network via time-bin-entanglement-based frequency conversion and Bell-state measurement

Zhantong Qi,^{1,2,*} Yilin Yang,^{2,*} Chennan Wu^{2,*}, Zixuan Liao,² Bo Tang,² Jiani Lei,² Yuanhua Li,^{1,2,†} Jia Lin^{2,‡}, Yuanlin Zheng,^{2,5,§} and Xianfeng Chen^{2,3,4,5,||}

¹*Department of Physics, Shanghai Key Laboratory of Materials Protection and Advanced Materials in Electric Power, Shanghai University of Electric Power, Shanghai 200090, China*

²*School of Physics and Astronomy, Shanghai Jiao Tong University, Shanghai 200240, China*

³*Shanghai Research Center for Quantum Sciences, Shanghai 201315, China*

⁴*Collaborative Innovation Center of Light Manipulations and Applications, Shandong Normal University, Jinan 250358, China*

⁵*Hefei National Laboratory, Hefei 230088, China*



(Received 14 November 2024; revised 1 April 2025; accepted 29 April 2025; published 12 May 2025)

Large-scale quantum communication systems often require different channels to be connected to multiple networks via frequency conversion, which requires frequency converters to act as relay points for system connectivity. We propose a quantum network for single-photon frequency conversion based on time-bin entanglement, where legitimate users can realize the spanning of communication bands between users by independently choosing the target conversion frequency mode. The results show that the converter in the network can be used as a bridge to completely connect the two networks by cascading the quadratic nonlinear process. Meanwhile, the converted quantum entangled states are demonstrated in entanglement measurements and can be used for entanglement swapping. This scheme is expected to be widely used in scenarios where different networks share quantum resources, switching communication channels and effectively connecting different multiplexed spectrum. This concept also provides significant applications in large-scale metropolitan area networks.

DOI: [10.1103/PhysRevA.111.052609](https://doi.org/10.1103/PhysRevA.111.052609)

I. INTRODUCTION

The future quantum network will be a scalable, secure, and fully connected network and should integrate different transmission links, such as satellite communication, ground-based free space communication, and long-distance fiber optic communication links [1,2]. In recent years, fully connected quantum communication networks based on quantum entanglement have attracted much attention in the construction of large-scale metropolitan area networks, such as quantum key distribution (QKD) networks [3–5], quantum entanglement distribution networks [6,7], and quantum secure direct communication networks [8]. However, in these networks, as the number of users increases, the number of quantum correlations and communication links increases and the structure gets more complex. The establishment of large-scale networks relies on a large number of quantum repeaters [9,10] whose core technology is quantum entanglement swapping (QES) [11–13], which can realize the entanglement of uncorrelated users in the network and the entanglement of global users to implement quantum communication. Presently, there are two methods to realize QES: linear Bell-state measurement (BSM) [14] and nonlinear BSM [15,16]. As shown in

Fig. 1(a), linear BSM assisted with postselection can realize the entanglement of the nonentangled users in the networks. This method demands the identity of the frequency of the two photons in the BSM, limiting the realization of entanglement distribution technology. As shown in Fig. 1(b), nonlinear BSM can achieve deterministic QES. Based on the sum-frequency generation (SFG) of two single photons at different frequencies, the entanglement of uncorrelated photons can be realized. However, because the efficiency of the SFG of single photons is only 10^{-8} , this scheme is not competent for constructing interconnection between long-distance quantum communication networks. Obviously, these two methods are both unsuitable for large-scale quantum entanglement networks. Fortunately, as shown in Fig. 1(c), we find that the QES based on single-photon frequency conversion (SPFC) and linear BSM may realize the fusion of frequency-unmatched quantum networks. The SPFC via cascaded quadratic nonlinear processes can convert photons of different frequencies into the same frequency for linear BSM [17,18]. Common methods for spontaneous parametric down-conversion (SPDC) include sum-frequency and difference-frequency generation [19] and electro-optic modulation [20,21] based on second-order nonlinear effects, and Bragg scattering four-wave mixing [22,23] based on third-order nonlinear effects. Electro-optic modulation is limited by the frequency of electrical signals and cannot achieve SPFC of hundreds of gigahertz, while Bragg scattering four-wave mixing based on third-order nonlinear effects requires high pump laser intensity to achieve high conversion efficiency. The nonlinear cascading process overcomes these limitations,

*These authors contributed equally to this work.

†Contact author: lyhua1984@shiep.edu.cn

‡Contact author: jlin@shiep.edu.cn

§Contact author: ylzheng@sjtu.edu.cn

||Contact author: xfchen@sjtu.edu.cn

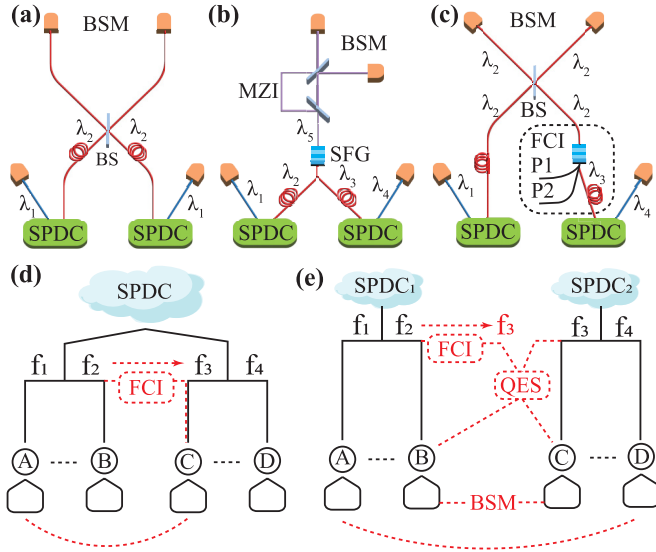


FIG. 1. The concept of the BSM and entanglement-swapping-based FCI and DWDM network. (a) Linear BSM. (b) Nonlinear BSM. (c) Single-photon frequency conversion and linear BSM. (d) FCI-based user association under the same SPDC source. (e) FCI-based user association under different SPDC sources.

and in this work, using only 6.8 mW of pump laser power, we achieve a conversion efficiency of 64.5% for SPFC of hundreds of gigahertz. Combining SPFC and linear BSM can realize the entanglement of any two users in the networks, performing different quantum information processing assignments

Here, we propose a quantum communication network based on SPFC and linear BSM. In this network, single-photon sources distribute telecom photons to different users based on dense wavelength division multiplexing (DWDM), where each user holds photons from one specific channel. The interuser connection scheme within a subnet under the same SPDC source is illustrated in Fig. 1(d), where the SPDC source distributes entangled photon pairs $f_1 - f_2$ and $f_3 - f_4$, with Alice holding f_1 , Bob holding f_2 , Chole holding f_3 , and Dave holding f_4 . When originally unassociated users need to communicate (e.g., Alice with f_1 and Chole with f_3), the frequency conversion interface (FCI) can convert the f_2 photon associated with f_1 into an f_3 photon and distribute it to Chole, thereby establishing a connection between Alice and Chole. The user connection scheme between different SPDC sources is shown in Fig. 1(e), where two SPDC sources independently distribute entangled photon pairs. When communication is required between Alice in SPDC₁ and Dave in SPDC₂, the f_2 photon can be converted to an f_3 photon via FCI, followed by entanglement swapping with the f_3 photon held by Chole in SPDC₂. Through BSM implementation, the connection between Alice and Dave can be established. The FCI-based user entanglement scheme proposed in this work is not limited to the illustrated network architecture, but can in principle be applied to any entanglement-based quantum communication network, with no dependence on photon frequencies. Our scheme applies to global unconnected users achieving quantum entanglement to perform various quantum communication tasks.

II. EXPERIMENT

As shown in Fig. 1, to realize the fusion of frequency-unmatched quantum networks, we list three different QES methods. Through comparison, we find that the BSM based on the combination of SPFC and linear BSM methods is the best proposal for constructing large-scale quantum communication networks and large-scale connections between uncorrelated users. Our design for the quantum communication network based on SPFC and linear entanglement swapping is presented in Figs. 1(d) and 1(e), where SPDC-entangled photon sources generate time-bin-entangled photon pairs and distribute photons to distant users in each subnet. Each user receives single quantum states at a specific wavelength. All users are in a fully connected network after performing SPFC and linear entanglement swapping based on fourfold Hong-Ou-Mandel (HOM) interference. Therefore, the way of building a network is linearly increasing and does not depend on the number of users. We can easily achieve communication between any two users.

Next, we experimentally demonstrate the feasibility of our approach. In the experiment, three SPDC single-photon sources distribute three time-bin-entangled photon pairs to six users, where each user possesses one photon at a certain frequency. To realize the fusion of subnets, a multiple-frequency 60-MHz femtosecond laser is split into four channels through a 100-GHz DWDM. The CH39 is the pump light for producing single photons and time-bin entanglement states. CH07, CH08, and CH09 (wavelengths of 1571.85, 1571.04, and 1570.2 nm, respectively) are the pump light for SPFC. Photons in CH39 pass through an unbalanced Mach-Zehnder interferometer (MZI) to produce double pulses with a delay time of 1 ns, where the time modes t_0 and t_1 represent the short and long arms, respectively, amplified by an erbium-doped optical fiber amplifier (EDFA), producing frequency-doubled photons in the first periodically poled lithium niobate (PPLN). Then it is divided into three paths, and each path is connected with a PPLN for SPDC. After passing through a 180-dB wavelength division multiplexing (WDM), 100-GHz DWDM is used to produce single photons. Then, the single-photon pairs generated in the SPDC are time-bin entangled, and these six single photons are distributed to six users. Each user implies a single photon detector (SPD) for detection and coincidence measurement. In our experiment, the six photon channels are CH21, CH22, CH23, CH56, CH57, and CH58. As shown in Fig. 2(a), CH21 and CH57, CH22 and CH56, and CH23 and CH55 are three pairs of correlated photons, passing through two unbalanced MZI to be entangled. The entangled photon pairs can be written as $|\phi\rangle = 1/\sqrt{2}(|t_0\rangle|t_0\rangle + e^{2i\theta}|t_1\rangle|t_1\rangle)$. As shown in Fig. 2(b), we realize the BSM of photons of different frequencies with FCI, by measuring the photon count of fourfold coincidence, the visibility of HOM dip is obtained, and the visibility of the entangled state after QES is calculated. For example, when Dave (CH21) wants to communicate with Feng (CH22), photons in CH56 and CH57 need to undergo QES to build the entanglement between CH21 and CH22. In this case the CH21 in Fig. 2(a) should be connected to port A in Fig. 2(b), CH56 to B, CH57 to C, and CH22 to D, and the pump lights P1 and P2 are from CH08 and CH09, respectively. In order to improve the visibility of our HOM interference, the

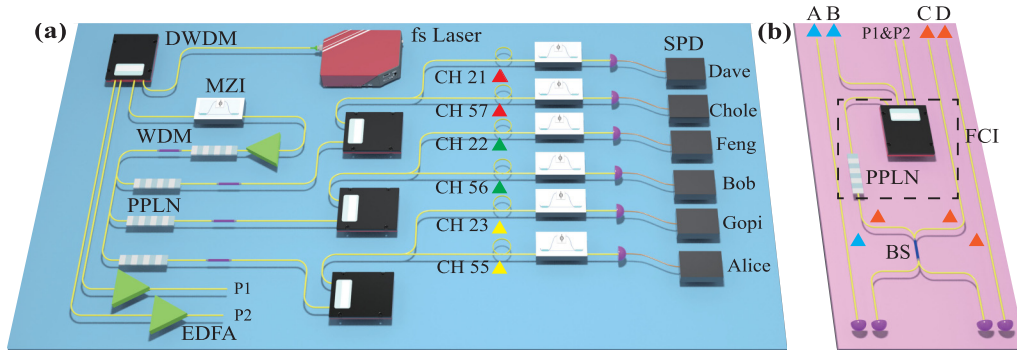


FIG. 2. Experiment setup. (a) The network distribution architecture for the steps of multiplexing and demultiplexing. (b) Fourfold HOM interference.

photons in CH56 (or CH57) are all filtered by a narrow-band filter with a bandwidth of 0.1 nm before SPFC.

In our experiment, we can achieve efficient SPFC based on a second-order nonlinear cascade process, and we implement a 5.2-cm-long PPLN waveguide with a polarization period of 19 μm , taking advantage of the type-0 quasi-phase matching (QPM) configuration in the telecom band and its low dispersion property. The conversion efficiency η_c can be expressed as [17]

$$\eta_c(L) = \frac{\eta_1 \eta_2 P_{p1} P_{p2} |\cos[2(\varphi_1 - \varphi_2)]|}{(\eta_1 P_{p1} + \eta_2 P_{p2})^2} \times \{1 - \cos[(\eta_1 P_{p1} + \eta_2 P_{p2})^{(1/2)} L]\}^2, \quad (1)$$

where η_1 and η_2 are the normalized power efficiencies and $\eta_1 \approx \eta_2 = 0.028 \text{ mW cm}^2$, P_{p1} , and P_{p2} are the powers of the pump laser in the SPFC, φ_1 and φ_2 are the phases of these two pumps, and L is the length of the PPLN waveguide. Perfect SPFC can be obtained when $P_{p1} = P_{p2} = \pi^2 / (2\eta_1 L^2)$; we calculate this result when both pump lasers are at 6.5 mW. Due to the limitation of the input power of the waveguide, the conversion efficiency of this cascade process is also restricted. In theory, we can achieve perfect efficiency of SPFC.

III. RESULTS AND DISCUSSION

The PPLN waveguide we utilize has a weak dispersion at telecom wavelengths, and the width of the spectrum is about 70 nm, covering the entire telecom C-band as shown in Fig. 3(a). The theoretical curve was calculated from the Sellmeier coefficients of Ref. [24]. The spectrum of correlated photon pairs is symmetric concerning a central wavelength of 1545.9 nm. To obtain the efficiency of FCI, then we can transform the wavelength of the signal photon to another communication wavelength through the frequency converter cascading the SFG and difference-frequency generation (DFG) process. Three pump wavelengths (CH07, CH08, and CH09) are isolated for signal photon conversion in the pulsed laser to be selected. After amplifying to a total power of about 6.8 mW, these pumps are filtered through a bandpass of about 150 dB to eliminate any amplifier noise near the photon frequency. The variation of conversion efficiency with total pump power is shown in Fig. 3(b). Each user is equipped with a suite of detection and processing modules, including

a 1-GHz unbalanced MZI and a SPD. By using the random detection of photons on a time basis and energy basis, end users can extract the security key information from the local measurement results of entangled photon pairs according to the Bennett-Brassad-Mermin 92 protocol (BBM92) [25] and realize the communication transmission between networks. To characterize the performance of the constructed network, we first measured the coincidence counts between users' entanglement distribution. The measured results of coincidence events between users are shown in the unshaded area on the left of Fig. 4. The average power of the second harmonic is 5 mW, which corresponds to a single-photon count rate of more than $10^3/\text{s}$. The PPLN is kept at 67.5 $^\circ\text{C}$ to achieve optimal type-0 QPM, which takes advantage of its weak dispersion properties in the telecommunication band to allow simultaneous phase matching of cascaded SFG and DFG processes over a wide bandwidth. At the same time, each user's SPD is set to synchronize with the laser pulse. The SPD detection efficiency is about 10% and the dark count rate is 1×10^{-6} per gate. The detection events of SPD are recorded by a single photon count with a time-to-digital correlator to calculate the coincidences. The conversion efficiency reaches up to 64.5% when the total pump power is 6.8 mW. As shown in the right of Fig. 4, we obtain the coincidental event measurements after SPFC.

Another important property of the converter is that it maintains the quantum properties of the signal photons during the transformation process. To demonstrate this property, we need to confirm that high-quality entanglements are allocated to

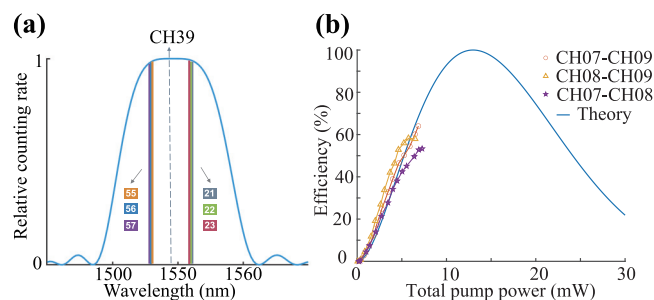


FIG. 3. (a) Spectrum of an SPDC source based on a PPLN waveguide. (b) Variation of conversion efficiency for three different pump combinations.

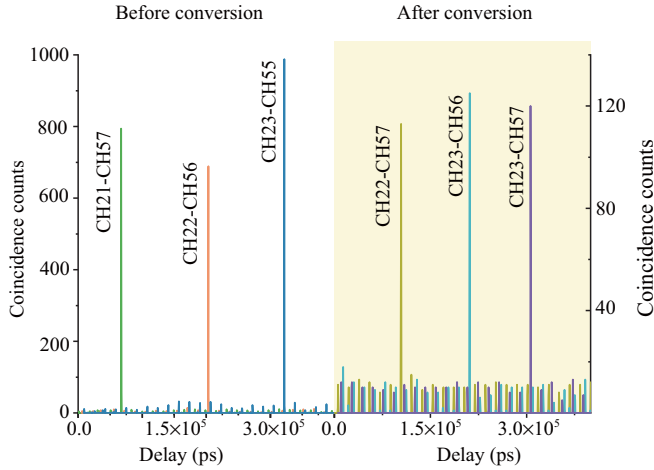


FIG. 4. Results of coincidence counts before and after frequency conversion between users.

all available channels assigned to each user. We measure the correlation and visibility of photon pairs after FCI and after BSM, respectively. The CH55 photons in the original SPDC photon pairs (CH23-CH55) are converted to CH57 photon through SPFC, the coincidence counts between the converted CH57 photon and the CH23 photon were then measured, and the entanglement visibility of the CH57-CH53 photon pair was obtained. The result is shown in the CH23-CH57 bar in Fig. 4 and the CH23-CH57 bar in Fig. 5(d), confirming that SPFC did not alter the correlation properties of the photons. We measure the entanglement between the signal and the idler photon, characterizing the quality of time-bin entanglement by conducting a Franson-type measurement [26] experiment of CH23 and CH55 from the SPDC source as shown in Fig. 5(a), and CH23 from the SPDC source and CH57, which is converted from CH55 by FCI as shown in

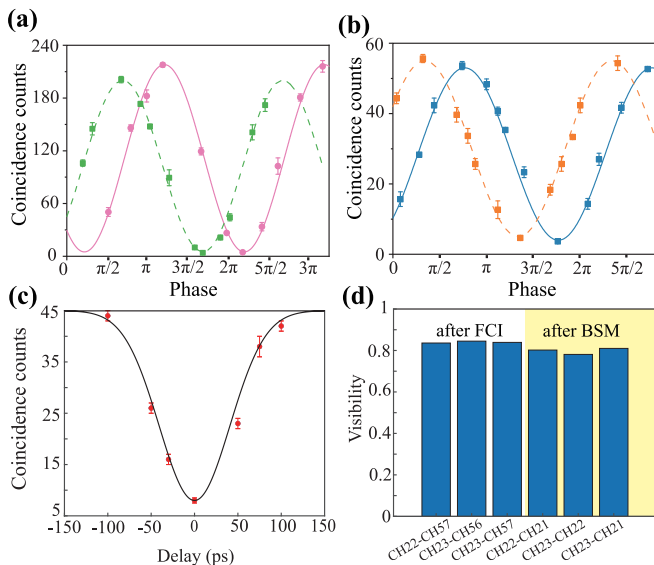


FIG. 5. Experimental results. (a) Typical two-photon interference fringe before SPFC. (b) After SPFC. (c) Fourfold HOM dip. (d) Visibility of the entanglement states.

Fig. 5(b). If the relative path delay between the two arms of MZI is less than the coherence length, the interference fringe can be observed by scanning the relative phase of an MZI. We perform Franson-type measurement based on superposition by scanning the phase in the idler interferometer and controlling the phase in two nonorthogonal signal interferometers by adjusting the voltage of the MZI device. Then, we obtain an average visibility before and after the SPFC calculated as $V = (N_{\max} - N_{\min}) / (N_{\max} + N_{\min}) = 95.49\% \pm 1.27\%$ and $83.6\% \pm 1.37\%$, exceeding the nonlocal bound of the Bell inequality $1/\sqrt{2}$, entangling the CH23 with CH57. Therefore, photon pairs can still be used for quantum communication tasks. The pump itself may also produce second harmonics or experience SFG between them, and these new frequencies can generate noise photons through the SPDC. The main source of noise is Raman scattering. To avoid this unexpected interaction, we chose pumps far away from the signal and target frequency to reduce their impact and effectively filter out the noise caused by the pump [27]. In the same way, we can realize the entanglement between CH22 and CH57 and between CH23 and CH56 by converting CH56 into CH57 and CH55 into CH56, respectively. As shown in Fig. 5(d), we can obtain the visibility of the other three entanglement states after FCI. It can be proven that the visibility of the new entangled states generated by the QES is the same as the visibility of the entangled states measured by our fourfold coincidence, therefore we can interfere with the same frequency photons by attenuating the channel. Then, we perform a fourfold coincidence measurement through photon interference of the same frequency, and obtain the visibility of uncorrelated photon pairs according to the size of the coincidence count, as shown in Fig. 5(c). By interfering with the CH57 photons generated after the FCI and the CH57 photons generated by the SPDC, the fourfold HOM dip is measured by the coincidence-counting method and the measurement time of each point is 10 h. We can obtain the entanglement visibility of uncorrelated photon pairs CH22-CH21. The same method is used to obtain the entangled photon contrast of uncorrelated photon pairs CH23-CH22 and CH23-CH21, as shown in Fig. 5(d). These results prove that entanglement can be generated between the uncorrelated users and all the users can communicate with each other by an entanglement-based QKD protocol.

We theoretically simulate QKD between users by using the standard BBM92 protocol in the time-bin-entangled network. According to the protocol, the users obtain the raw keys by filtering the coincidence events by the photons detected on the same basis. The raw keys need to go through postprocessing processes such as error correction and privacy amplification to obtain a secure key. According to Koashi and Preskill's security proof [28], the generation rate of a secure key rate is $R \geq Q[1 - fH(e_b) - H(e_p)]$, where Q is the original key generation rate; $f = 1.16$ is the error correction efficiency; e_b and e_p denote the bit error rate and phase error rate, respectively; and $H(x) = -x \log_2(x) - (1-x) \log_2(1-x)$ is the Shannon binary entropy function. The value of the bit error rate can be measured directly experimentally by utilizing the two-photon interference visibility V as $e_p = \frac{1-V}{2}$ [29,30]. In the system, we choose the data postprocessing process for two-way classical communication with a higher threshold of

error rate tolerance [31,32]. Time-bin entanglement as a discrete mode of time-energy entanglement, can directly encode quantum information within the arrival time of a photon [30]. As well as the standard entanglement-based QKD protocol, quantum internet tasks such as distributed quantum computing [33], quantum teleportation [16,34], and quantum secret sharing [35–37] can be implemented on our network.

IV. CONCLUSION

In conclusion, we have demonstrated SPFC based on time-bin-entangled quantum networks. In our proposed scheme, users in the network can actively select pumps to efficiently switch their single-photon frequency between DWDM channels, which in turn connects network users occupying different bands. Moreover, the time-bin entanglement is well maintained during the SPFC and linear BSM process. We note that this scheme can be used for internetwork communication

band switching, expanding with multinet network connections as wavelength bridges. Therefore, our scheme has the potential to realize a scalable multinet network with low-noise connection.

ACKNOWLEDGMENTS

This work is supported in part by the National Natural Science Foundation of China (Grants No. 12074155, No. 62375164, and No. 12192252), the Foundation for Shanghai Municipal Science Technology Major Project (Grant No. 2019SHZDZX01-ZX06), SJTU (No. 21X010200828), Innovation Programme for Quantum Science and Technology (Grant No. 2021ZD0300802), the Shuguang Program of Shanghai Education Development Foundation and Shanghai Municipal Education Commission (Grant No. 24SG53), and Guangdong Provincial Quantum Science Strategic Initiative (Grant No. GDZX2403003).

-
- [1] L. Yu, C. M. Natarajan, T. Horikiri, C. Langrock, J. S. Pelc, M. G. Tanner, E. Abe, S. Maier, C. Schneider, S. Höfling, M. Kamp, R. H. Hadfield, M. M. Fejer, and Y. Yamamoto, Two-photon interference at telecom wavelengths for time-bin-encoded single photons from quantum-dot spin qubits, *Nat. Commun.* **6**, 8955 (2015).
- [2] C. Simon, Towards a global quantum network, *Nat. Photon.* **11**, 678 (2017).
- [3] W. Li, L. Zhang, H. Tan, Y. Lu, S.-K. Liao, J. Huang, H. Li, Z. Wang, H.-K. Mao, B. Yan, Q. Li, Y. Liu, Q. Zhang, C.-Z. Peng, L. You, F. Xu, and J.-W. Pan, High-rate quantum key distribution exceeding 110 Mb s⁻¹, *Nat. Photon.* **17**, 416 (2023).
- [4] W. Zhang, T. van Leent, K. Redeker, R. Garthoff, R. Schwonnek, F. Fertig, S. Eppelt, W. Rosenfeld, V. Scarani, C. C.-W. Lim, and H. Weinfurter, A device-independent quantum key distribution system for distant users, *Nature (London)* **607**, 687 (2022).
- [5] W.-Z. Liu, Y.-Z. Zhang, Y.-Z. Zhen, M.-H. Li, Y. Liu, J. Fan, F. Xu, Q. Zhang, and J.-W. Pan, Toward a photonic demonstration of device-independent quantum key distribution, *Phys. Rev. Lett.* **129**, 050502 (2022).
- [6] S. P. Neumann, A. Buchner, L. Bulla, M. Bohmann, and R. Ursin, Continuous entanglement distribution over a transnational 248 km fiber link, *Nat. Commun.* **13**, 6134 (2022).
- [7] F. B. Basset, M. Valeri, E. Rocca, V. Muredda, D. Poderini, J. Neuwirth, N. Spagnolo, M. B. Rota, G. Carvacho, F. Sciarrino, and R. Trotta, Quantum key distribution with entangled photons generated on demand by a quantum dot, *Sci. Adv.* **7**, eabe6379 (2021).
- [8] Z. Qi, Y. Li, Y. Huang, J. Feng, Y. Zheng, and X. Chen, A 15-user quantum secure direct communication network, *Light Sci. Appl.* **10**, 183 (2021).
- [9] Z.-D. Li, R. Zhang, X.-F. Yin, L.-Z. Liu, Y. Hu, Y.-Q. Fang, Y.-Y. Fei, X. Jiang, J. Zhang, L. Li, N.-L. Liu, F. Xu, Y.-A. Chen, and J.-W. Pan, Experimental quantum repeater without quantum memory, *Nat. Photon.* **13**, 644 (2019).
- [10] K. Azuma, K. Tamaki, and H.-K. Lo, All-photonic quantum repeaters, *Nat. Commun.* **6**, 6787 (2015).
- [11] E. Shchukin and P. Van Loock, Optimal entanglement swapping in quantum repeaters, *Phys. Rev. Lett.* **128**, 150502 (2022).
- [12] C.-X. Huang, X.-M. Hu, Y. Guo, C. Zhang, B.-H. Liu, Y.-F. Huang, C.-F. Li, G.-C. Guo, N. Gisin, C. Branciard, and A. Tavakoli, Entanglement swapping and quantum correlations via symmetric joint measurements, *Phys. Rev. Lett.* **129**, 030502 (2022).
- [13] F. Basso Basset, M. B. Rota, C. Schimpf, D. Tedeschi, K. D. Zeuner, S. F. Covre da Silva, M. Reindl, V. Zwiller, K. D. Jöns, *et al.*, Entanglement swapping with photons generated on demand by a quantum dot, *Phys. Rev. Lett.* **123**, 160501 (2019).
- [14] Q.-C. Sun, Y.-F. Jiang, Y.-L. Mao, L.-X. You, W. Zhang, W.-J. Zhang, X. Jiang, T.-Y. Chen, H. Li, Y.-D. Huang, X.-F. Chen, Z. Wang, J. Fan, Q. Zhang, and J.-W. Pan, Entanglement swapping over 100 km optical fiber with independent entangled photon-pair sources, *Optica* **4**, 1214 (2017).
- [15] N. Sangouard, B. Sanguinetti, N. Curtz, N. Gisin, R. Thew, and H. Zbinden, Faithful entanglement swapping based on sum-frequency generation, *Phys. Rev. Lett.* **106**, 120403 (2011).
- [16] Y. Li, Y. Huang, T. Xiang, Y. Nie, M. Sang, L. Yuan, and X. Chen, Multiuser time-energy entanglement swapping based on dense wavelength division multiplexed and sum-frequency generation, *Phys. Rev. Lett.* **123**, 250505 (2019).
- [17] T. Xiang, Q.-C. Sun, Y. Li, Y. Zheng, and X. Chen, Single-photon frequency conversion via cascaded quadratic nonlinear processes, *Phys. Rev. A* **97**, 063810 (2018).
- [18] P. Fisher, R. Cernansky, B. Haylock, and M. Lobino, Single photon frequency conversion for frequency multiplexed quantum networks in the telecom band, *Phys. Rev. Lett.* **127**, 023602 (2021).
- [19] X. Wang, X. Jiao, B. Wang, Y. Liu, X.-P. Xie, M.-Y. Zheng, Q. Zhang, and J.-W. Pan, Quantum frequency conversion and single-photon detection with lithium niobate nanophotonic chips, *npj Quantum Inf.* **9**, 38 (2023).
- [20] L. Olislager, E. Woodhead, K. Phan Huy, J.-M. Merolla, P. Emplit, and S. Massar, Creating and manipulating entangled optical qubits in the frequency domain, *Phys. Rev. A* **89**, 052323 (2014).

- [21] H.-H. Lu, J. M. Lukens, M. Alshowkan, B. T. Kirby, and N. A. Peters, Building a controlled-NOT gate between polarization and frequency, *Optica Quantum* **2**, 282 (2024).
- [22] S. Clemmen, A. Farsi, S. Ramelow, and A. L. Gaeta, Ramsey interference with single photons, *Phys. Rev. Lett.* **117**, 223601 (2016).
- [23] A. S. Clark, S. Shahnian, M. J. Collins, C. Xiong, and B. J. Eggleton, High-efficiency frequency conversion in the single-photon regime, *Opt. Lett.* **38**, 947 (2013).
- [24] O. Gayer, Z. Sacks, E. Galun, and A. Arie, Temperature and wavelength dependent refractive index equations for MgO-doped congruent and stoichiometric LiNbO₃, *Appl. Phys. B* **94**, 367 (2009).
- [25] C. H. Bennett, G. Brassard, and N. D. Mermin, Quantum cryptography without Bell's theorem, *Phys. Rev. Lett.* **68**, 557 (1992).
- [26] O. Kwon, K.-K. Park, Y.-S. Ra, Y.-S. Kim, and Y.-H. Kim, Time-bin entangled photon pairs from spontaneous parametric down-conversion pumped by a cw multi-mode diode laser, *Opt. Express* **21**, 25492 (2013).
- [27] P. Fisher, M. Villa, F. Lenzini, and M. Lobino, Integrated optical device for frequency conversion across the full telecom *c*-band spectrum, *Phys. Rev. Appl.* **13**, 024017 (2020).
- [28] M. Koashi, Simple security proof of quantum key distribution based on complementarity, *New J. Phys.* **11**, 045018 (2009).
- [29] F. Xu, X. Ma, Q. Zhang, H.-K. Lo, and J.-W. Pan, Secure quantum key distribution with realistic devices, *Rev. Mod. Phys.* **92**, 025002 (2020).
- [30] J.-H. Kim, J.-W. Chae, Y.-C. Jeong, and Y.-H. Kim, Quantum communication with time-bin entanglement over a wavelength-multiplexed fiber network, *APL Photon.* **7**, 016106 (2022).
- [31] D. Gottesman and H.-K. Lo, Proof of security of quantum key distribution with two-way classical communications, *IEEE Trans. Inf. Theory* **49**, 457 (2003).
- [32] Q.-C. Sun, Y.-L. Mao, Y.-F. Jiang, Q. Zhao, S.-J. Chen, W. Zhang, W.-J. Zhang, X. Jiang, T.-Y. Chen, L.-X. You, L. Li, Y.-D. Huang, X.-F. Chen, Z. Wang, X. Ma, Q. Zhang, and J.-W. Pan, Entanglement swapping with independent sources over an optical-fiber network, *Phys. Rev. A* **95**, 032306 (2017).
- [33] D. Cuomo, M. Caleffi, and A. S. Cacciapuoti, Towards a distributed quantum computing ecosystem, *IET Quantum Commun.* **1**, 3 (2020).
- [34] S. Pirandola, J. Eisert, C. Weedbrook, A. Furusawa, and S. L. Braunstein, Advances in quantum teleportation, *Nat. Photon.* **9**, 641 (2015).
- [35] S. M. Lee, S.-W. Lee, H. Jeong, and H. S. Park, Quantum teleportation of shared quantum secret, *Phys. Rev. Lett.* **124**, 060501 (2020).
- [36] H. Lu, Z. Zhang, L.-K. Chen, Z.-D. Li, C. Liu, L. Li, N.-L. Liu, X. Ma, Y.-A. Chen, and J.-W. Pan, Secret sharing of a quantum state, *Phys. Rev. Lett.* **117**, 030501 (2016).
- [37] Y. Zhou, J. Yu, Z. Yan, X. Jia, J. Zhang, C. Xie, and K. Peng, Quantum secret sharing among four players using multipartite bound entanglement of an optical field, *Phys. Rev. Lett.* **121**, 150502 (2018).